THE VARIETY OF FAHLORES AND THE EPIGENETIC MINERALS FROM THE LEBEDINOE DEPOSIT

Svetlana N. Nenasheva, Leonid A. Pautov, Vladimir Y. Karpenko
Fersman Mineralogical Museum, Russian Academy of Sciences, Moscow, nenashevasn@mail.ru

The new results of the mineralogical study of the Lebedinoe deposit are discussed. In addition to Zn-bearing tetrahedrite (sandbergerite), tetrahedrite-tennantite, and tennantite (Nenasheva *et al.*, 2010), Te-bearing fahlores (goldfieldite-tennantite-tetrahedrite, goldfieldite-tennantite, and Te-bearing tennantite-tetrahedrite), tetrahedrite with significant Ag, and anisotropic tetrahedrite-tennantitewere identified. These minerals were found in varied assemblages, whose mineral composition indicate the conditions of ore formation: the composition of mineral-forming fluid, temperature, and pH value. The chalcocite polysomatic series minerals, digenite, anilite, spionkopite, and yarrowite, used as geothermometer were discovered in the ores.
7 figures, 9 tables, 17 references.
Keywords: fahlores, bournonite, hessite, petzite, anilite, spionkopite, yarrowite, bayldonite, clinotyrolite, strashimirite, leogangite, Lebedinoe deposit.

Introduction

Nenasheva *et al.* (2010) characterized in detail the Lebedinoe deposit. The deposit is reported according to Fastalovich and Petrovskaya (1940) and Petrovskaya (1973). Below is very brief description of the deposit. Weakly metamorphosed Cambrian dolomite overlapping eroded granite is intruded by Upper Jurassic to Lower Cretaceous numerous small intrusions. These are predominantly intermediate stocks, laccoliths, and dikes with elevated alkalinity. The metasomatic sulfide-carbonate bodies, occasionally as vein apophysises are hosted in dolomite along horizontal faults (Petrovskaya, 1973). Pyrite is dominant ore mineral; chalcopyrite is also occurs; in some veins, there is hematite. Galena, sphalerite, pyrrhotite, galenobismutite, tetrahedrite, native gold, bornite, cobaltite, and sulvanite are less frequent. Supergene minerals are iron hydroxides, jarosite, cuprite, chalcocite, covellite, malachite, azurite, cerussite, gypsum, and melanterite (Fastalovich, Petrovskaya, 1940; Nenasheva *et al.*, 2010).

Experimental and results

The thin polished sections were examined with an OPTON optical microscope. The chemical composition was determined with a CamScan-4D scanning electron microscope equipped with a Link ISIS energy dispersion system (EDS) operating at 20 kV and current absorbed at metallic cobalt of 4 nA. The X-ray powder diffraction patterns were recorded at an URS-50 diffractometer with an RKD 57.3 mm camera, Fe$K\alpha$-radiation, Mn filter. The sample was selected from thin polished section and mount in resin ball.

The optically heterogeneous objects studied are composed of ore minerals (pyrite, galena, and bornite are the major) submerged into quartz-carbonate-arsenate matrix. In addition, pyrrhotite, covellite, digenite, anilite, spionkopite, and yarrowite were identified with electron microprobe.

The names of fahlores are given according to Mozgova and Tsepin (1983). Sb-bearing fahlores are predominant. Tetrahedrite with significant Zn (sandbergerite) is associated with galena, famatinite, arsenosulvanite, anglesite, and copper arsenates: bayldonite, leogangite, and euchroite (Nenasheva *et al.*, 2010). Content of Zn ranges from 5.14 to 8.07 wt.% corresponding to 1.32 – 2.04 *apfu*. Ag is present in all compositions varying from 0.65 to 4.37 wt.% that corresponds to 0.10 – 0.68 *apfu*. Concentration of Sb ranges from 23.53 to 28.16 wt.% exceeding 3 *apfu* and corresponding to 3.25 – 3.85 *apfu* (Nenasheva *et al.*, 2010). There is no clear correlation between Zn and As. However, there is positive

Table 1. **Electron microprobe data (wt.%) of fahlores**

№ an.	Sample	Cu	Ag	Fe	Zn	Pb	Sb	As	Te	S	Se	Total
1	53/278(area 7)	41.58		0.01	6.68	0.56	14.68	7.40	2.59	25.44		98.94
2		46.27			2.69		5.75	8.73	10.77	25.98		100.19
3		45.37			1.61		7.16	5.89	12.83	25.44		98.30
4		47.27			1.62		5.18	6.90	11.83	25.68		98.48
5		47.21			3.36		4.78	9.23	9.48	26.03	0.36	100.45
6	53/278(area 6)	41.99			7.56		14.86	8.34	1.70	25.95		100.40
7*		44.73		0.14	3.36		7.66	7.23	9.25	26.00		98.37
8*		44.87			3.66		10.92	5.28	9.71	25.57		100.01
9*	53/278(area 4)	46.05			2.13		9.56	4.49	11.11	25.68		99.02
10*		47.26			2.29		8.96	5.91	10.34	26.60		101.36
11*		46.99			0.79		10.99	3.24	13.52	25.81		101.34
12*		46.13			3.12		9.58	4.72	10.26	25.04	0.69	99.54
13*		45.30			3.13		11.32	5.54	9.55	25.97		100.81
14*		45.49			2.86		8.25	7.62	10.26	27.15		101.63
15*		46.04			2.10		6.79	7.63	11.56	26.47		100.59
16*		46.33			2.38		7.99	6.75	11.04	25.30	0.36	100.15
17*		43.96			4.63		9.48	8.06	6.63	25.23	0.46	98.45
18**		42.62			8.74		9.21	12 88	0.77	26.43		100.65
19**		42.35			8.25		10.34	12.71	0.52	27.89		102.06
20**		42.10			7.58		8.61	13.75	0.75	27.44		100.23
21**		43.18			7.74		9.78	13.59	0.17	26.88		101.34
22**		43.46			7.16		8.67	12.18	2.28	26.43		100.18
23**		44.25			5.35		5.98	11.05	5.80	26.58		99.01
24**		44.32			4.67		5.78	11.93	5.52	26.33	0.64	99.19
25**		41.69			9.12		6.84	15.46	0.59	26.59		100.29
26**	53/278(area 6)	43.56			5.55		7.52	10.66	5.35	26.66		99.30
27**		44.04			5.45		10.80	7.84	5.30	26.47		99.90
28	2 (area 2)	34.89	4.93	4.52	2.92	0.87	27.31			24.33		99.77
29		35.63	4.26	4.02	3.37		27.47			24.62		99.37
30		35.45	4.79	4.84	2.61		27.60			24.49		99.78
31		36.66	3.44	4.58	3.18		23.67	2.31		24.91		98.75
32		35.83	4.87	4.90	2.64		24.94	1.28		24.89		99.35
33		36.15	3.62	4.52	3.50		23.84	2.50		24.87		99.00
34		35.62	3.69	4.72	3.06		24.28	2.07		24.37		97.81
35	2 (area 3)	35.46	2.88	4.12	2.99	2.14	25.10	1.30		23.50		97.49
36	242/1-2	41.13		0.62	7.79		18.01	7.20		25.88		100.63
37		41.68		0.43	8.31		18.50	7.07		26.59		102.58
38		41.05		0.38	8.22		18.84	7.26		25.88		101.63
39		41.65		0.32	8.63		18.81	6.87		25.93		102.21
40		41.79		0.47	8.56		13.17	10.37		26.74		101.10
41		41.68		0.40	7.83		15.03	9.44		26.81		101.19
42		41.54		0.33	8.09		16.36	8.59		26.22		101.13
43		39.49		1.42	7.11		18.73	6.00		25.26		98.01

*Notes: * — light zone, ** — dark zone. Analyses 1—35 were performed by V.Yu. Karpenko, anal. 36—43, by L.A. Pautov.*

correlation between Sb and Zn + Ag. Previously, Mozgova and Tsepin (1983) reported such correlation.

Tennantite-tetrahedrite and tennantite associated with sulvanite, arsenosulvanite, and Ca and Cu arsenate (tyrolite $Ca_2Cu^{2+}{}_5(OH,O)_4(AsO_4)_2(CO_3)\cdot 6H_2O$ or clinotyrolite $Ca_2Cu_9^{2+}(OH,O)_{10}[(AsO_4),(SO_4)]_4\cdot 10H_2O$) are characterized by negative correlation between As and Sb (Nenasheva *et al.*, 2010).

Te-bearing fahlores, goldfieldite-tennantite-tetrahedrite (Tables 1, 2; anal. 8, 9, 11—13), goldfieldite-tennantite-tetrahedrite (Tables 1, 2; anal. 2, 5, 7, 10, 14—17, 23, 24. 26, 27), and Te-bearing tennantite-tetrahedrite (Tables 1, 2; anal. 1, 6), and Te-bearing tetrahedrite-tennantite (Tables 1, 2; anal. 18—22) are associated with galena, quartz, native gold, secondary copper sulfides of the chalcocite, $mCu_2S \cdot nCuS$, polysomatic series, and copper arsenates. Fahlores occur as anhedral grains filling occasionally interstices between grains of quartz, galena, and pyrite and sometimes overgrowing quartz crystals (Fig. 1). Content of Te ranges from 0.17 to 13.52 wt.% corresponding to 0.02—1.71 *apfu*. Te-bearing

Table 2. **Formulae of fahlores calculated on the basis of 29 atoms in the unit cell**

№ an.	Sample	Formula	Δ, % — valence balance
1	53/278 (area 7)	$Cu_{10.00}(Cu_{0.58}Zn_{1.65}Pb_{0.04})_{2.27}(Sb_{1.95}As_{1.60}Te_{0.17})_{3.72}(S_{12.84}Te_{0.16})_{13.00}$	3.0
2		$Cu_{10.21}(Cu_{1.34}Zn_{0.66})_{2.00}(Sb_{0.75}As_{1.85}Te_{1.20})_{3.80}(S_{12.86}Te_{0.14})_{13.00}$	3.0
3		$Cu_{11.10}(Cu_{0.60}Zn_{0.40})_{1.00}(Sb_{0.96}As_{1.29}Te_{1.65})_{3.90}S_{13.00}$	1.7
4		$Cu_{10.41}(Cu_{1.60}Zn_{0.40})_{2.00}(Sb_{0.69}As_{1.49}Te_{1.42})_{3.60}(S_{12.92}Te_{0.08})_{13.00}$	2.4
5		$Cu_{10.47}(Cu_{1.19}Zn_{0.81})_{2.00}(Sb_{0.62}As_{1.93}Te_{0.98})_{3.53}(S_{12.74}Se_{0.07}Te_{0.19})_{13.00}$	0.2
6	53/278 (area 6)	$Cu_{10.29}(Cu_{0.17}Zn_{1.83})_{2.00}(Sb_{1.93}As_{1.76}Te_{0.21})_{3.90}S_{12.81}$	2.2
7*		$Cu_{10.21}(Cu_{1.13}Zn_{0.83}Fe_{0.04})_{2.00}(Sb_{1.01}As_{1.55}Te_{1.17})_{3.73}S_{13.06}$	1.7
8*		$Cu_{10.30}(Cu_{1.10}Zn_{0.90})_{2.00}(Sb_{1.45}As_{1.14}Te_{1.11})_{3.82}(S_{12.88}Te_{0.12})_{13.00}$	1.9
9*	53/278 (area 4)	$Cu_{10.31}(Cu_{1.47}Zn_{0.53})_{2.00}(Sb_{1.28}As_{0.97}Te_{1.42})_{3.67}S_{13.02}$	2.6
		$Cu_{11.31}(Cu_{0.47}Zn_{0.53})_{1.00}(Sb_{1.28}As_{0.97}Te_{1.42})_{3.67}S_{13.02}$	1.2
10*		$Cu_{10.26}(Cu_{1.45}Zn_{0.55})_{2.00}(Sb_{1.16}As_{1.24}Te_{1.28})_{3.68}S_{13.06}$	1.7
		$Cu_{11.26}(Cu_{0.45}Zn_{0.55})_{1.00}(Sb_{1.16}As_{1.24}Te_{1.28})_{3.68}S_{13.06}$	2.0
11*		$Cu_{10.13}(Cu_{1.81}Zn_{0.19})_{2.00}(Sb_{1.46}As_{0.70}Te_{1.71})_{3.87}S_{13.00}$	5.3
		$Cu_{11.13}(Cu_{0.81}Zn_{0.19})_{1.00}(Sb_{1.46}As_{0.70}Te_{1.71})_{3.87}S_{13.00}$	1.7
12*		$Cu_{10.57}(Cu_{1.22}Zn_{0.78})_{2.00}(Sb_{1.28}As_{1.02}Te_{1.30})_{3.60}(S_{12.68}Se_{0.14})_{12.82}$	3.9
		$Cu_{11.57}(Cu_{0.22}Zn_{0.78})_{1.00}(Sb_{1.28}As_{1.02}Te_{1.30})_{3.60}(S_{12.68}Se_{0.14})_{12.82}$	0.1
13*		$Cu_{10.17}(Cu_{1.24}Zn_{0.76})_{2.00}(Sb_{1.49}As_{1.18}Te_{1.20})_{3.87}S_{12.96}$	3.9
		$Cu_{11.57}(Cu_{0.24}Zn_{0.76})_{1.00}(Sb_{1.49}As_{1.18}Te_{1.20})_{3.87}S_{12.96}$	0.2
14*		$Cu_{10.00}(Cu_{1.18}Zn_{0.68})_{1.86}(Sb_{1.06}As_{1.59}Te_{1.26})_{3.91}S_{13.23}$	0.9
		$Cu_{11.00}(Cu_{0.18}Zn_{0.68})_{0.86}(Sb_{1.06}As_{1.59}Te_{1.26})_{3.91}S_{13.23}$	2.8
15*		$Cu_{10.00}(Cu_{1.48}Zn_{0.51})_{1.99}(Sb_{0.88}As_{1.61}Te_{1.43})_{3.92}S_{13.08}$	3.7
		$Cu_{11.00}(Cu_{0.48}Zn_{0.51})_{0.99}(Sb_{0.88}As_{1.61}Te_{1.43})_{3.92}S_{13.08}$	0.3
16*		$Cu_{10.32}(Cu_{1.42}Zn_{0.58})_{2.00}(Sb_{1.06}As_{1.45}Te_{1.39})_{3.90}(S_{12.70}Se_{0.07})_{12.77}$	6.8
		$Cu_{11.32}(Cu_{0.42}Zn_{0.58})_{1.00}(Sb_{1.06}As_{1.45}Te_{1.39})_{3.90}(S_{12.70}Se_{0.07})_{12.77}$	3.3
17*		$Cu_{11.19}Zn_{1.14}(Sb_{1.26}As_{1.74}Te_{0.84})_{3.84}(S_{12.73}Se_{0.10})_{12.83}$	0.6
18**		$Cu_{10.34}Zn_{2.06}(Sb_{1.16}As_{2.65}Te_{0.09})_{3.90}S_{12.70}$	3.2
		$Cu_{10.34}Zn_{2.06}(Sb_{1.16}As_{2.65})_{3.81}(S_{12.70}Te_{0.09})_{12.79}$	1.2
19**		$Cu_{10.00}(Cu_{0.06}Zn_{1.90})_{1.96}(Sb_{1.28}As_{2.56}Te_{0.06})_{3.90}S_{13.13}$	2.2
20**		$Cu_{10.00}(Cu_{0.14}Zn_{1.77})_{1.91}(Sb_{1.08}As_{2.81}Te_{0.09})_{3.98}S_{13.10}$	1.3
21**		$Cu_{10.19}(Cu_{0.19}Zn_{1.81})_{2.00}(Sb_{1.23}As_{2.77})_{4.00}(S_{12.80}Te_{0.02})_{12.82}$	2.1
		$Cu_{10.19}(Cu_{0.19}Zn_{1.81})_{2.00}(Sb_{1.23}As_{2.77}Te_{0.02})_{4.02}S_{12.80}$	2.6
22**		$Cu_{10.31}(Cu_{0.30}Zn_{1.70})_{2.00}(Sb_{1.10}As_{2.52}Te_{0.28})_{3.90}S_{12.79}$	2.7
		$Cu_{10.31}(Cu_{0.30}Zn_{1.70})_{2.00}(Sb_{1.10}As_{2.52}Te_{0.07})_{3.69}(S_{12.79}Te_{0.21})_{13.00}$	2.4
23**		$Cu_{10.20}(Cu_{0.72}Zn_{1.28})_{2.00}(Sb_{0.77}As_{2.31}Te_{0.71})_{3.79}S_{13.00}$	1.1
24**		$Cu_{10.06}(Cu_{0.88}Zn_{1.12})_{2.00}(Sb_{0.74}As_{2.50}Te_{0.68})_{3.92}(S_{12.88}Se_{0.13})_{13.01}$	1.8
25**		$Cu_{10.06}Zn_{2.14}(Sb_{0.86}As_{3.16})_{4.00}(S_{12.71}Te_{0.07})_{12.78}$	2.9
26**	53/278 (area 6)	$Cu_{10.09}(Cu_{0.67}Zn_{1.33})_{2.00}(Sb_{0.97}As_{2.23}Te_{0.66})_{3.86}S_{13.05}$	1.2
27**		$Cu_{10.26}(Cu_{0.68}Zn_{1.32})_{2.00}(Sb_{1.40}As_{1.65}Te_{0.66})_{3.71}S_{13.04}$	0.1
28	2 (area 2)	$(Cu_{9.32}Ag_{0.78})_{10.10}(Fe_{1.37}Zn_{0.76}Pb_{0.07})_{2.20}Sb_{3.81}S_{12.88}$	0.6
29		$(Cu_{9.47}Ag_{0.67})_{10.14}(Fe_{1.22}Zn_{0.87})_{2.09}Sb_{3.81}S_{12.96}$	0.6
30		$(Cu_{9.41}Ag_{0.75})_{10.16}(Fe_{1.46}Zn_{0.67})_{2.13}Sb_{3.82}S_{12.88}$	0.5
31		$(Cu_{9.61}Ag_{0.53})_{10.14}(Fe_{1.36}Zn_{0.81})_{2.17}(Sb_{3.24}As_{0.51})_{3.75}S_{12.93}$	0.5
32		$(Cu_{9.42}Ag_{0.75})_{10.17}(Fe_{1.46}Zn_{0.68})_{2.14}(Sb_{3.42}As_{0.29})_{3.71}S_{12.97}$	1.4
33		$(Cu_{9.47}Ag_{0.56})_{10.03}(Fe_{1.35}Zn_{0.89})_{2.24}(Sb_{3.25}As_{0.56})_{3.81}S_{12.91}$	0.5
34		$(Cu_{9.49}Ag_{0.58})_{10.07}(Fe_{1.43}Zn_{0.79})_{2.22}(Sb_{3.38}As_{0.47})_{3.85}S_{12.86}$	1.3
35	2 (area 3)	$(Cu_{9.69}Ag_{0.46})_{10.15}(Fe_{1.28}Zn_{0.79}Pb_{0.18})_{2.25}(Sb_{3.58}As_{0.30})_{3.88}S_{12.72}$	3.0
36	242/1-2	$Cu_{10.27}(Zn_{1.89}Fe_{0.18})_{2.07}(Sb_{2.35}As_{1.52})_{3.87}S_{12.80}$	1.6
37		$Cu_{10.19}(Zn_{1.97}Fe_{0.12})_{2.09}(Sb_{2.36}As_{1.46})_{3.82}S_{12.89}$	0.2
38		$Cu_{10.20}(Zn_{1.99}Fe_{0.11})_{2.10}(Sb_{2.44}As_{1.53})_{3.97}S_{12.74}$	3.1
39		$Cu_{10.29}(Zn_{2.07}Fe_{0.09})_{2.16}(Sb_{2.42}As_{1.44})_{3.86}S_{12.69}$	3.0
40		$Cu_{10.15}(Zn_{2.02}Fe_{0.13})_{2.15}(Sb_{1.67}As_{2.14})_{3.81}S_{12.88}$	0.5
41		$Cu_{10.18}(Zn_{1.86}Fe_{0.11})_{1,97}(Sb_{1.92}As_{1.95})_{3.87}S_{12.97}$	0.8
42		$Cu_{10.24}(Zn_{1.94}Fe_{0.09})_{2.03}(Sb_{2.10}As_{1.80})_{3.90}S_{12.82}$	1.4
43		$Cu_{10.14}(Zn_{1.77}Fe_{0.41})_{2.18}(Sb_{2.51}As_{1.31})_{3.82}S_{12.85}$	1.0

Notes: * *— light zone,* ** *— dark zone. Compositions 1 and 6 correspond to Te-bearing tennantite-tetrahedrite, 18—22, to Te-bearing tetrahedrite-tennantite, 2—5, 7, 10, 14—17, 23, 24, 26, and 27, to goldfieldite-tetrahedrite-tennantite, 8, 9, 11 13, to goldfieldite tennantite-tetrahedrite, 25, to tennantite, 28—35, to tetrahedrite, 36—39, 41—43, to anisotripic tennantite-tetrahedrite, and 40, to tetrahderite-tennantite.*

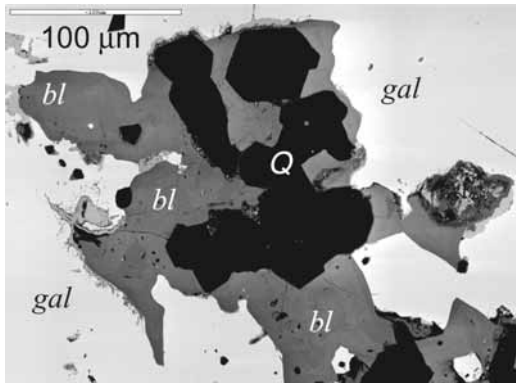

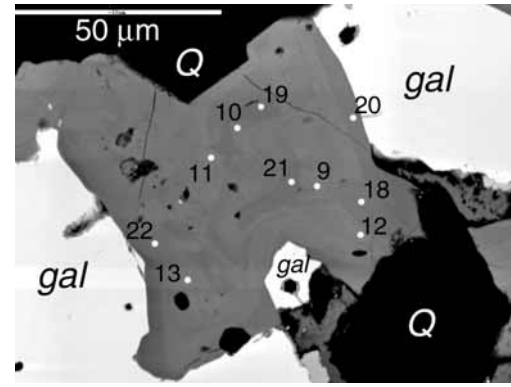

Fig. 1. Te-bearing fahlore overgrowing crystals of quartz. Quartz is black; fahlore is grey; and galena is light grey (BSE-image). Sample 53/278, area 4.

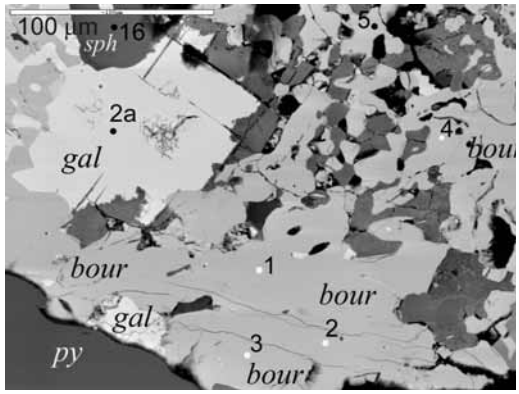

Fig. 2. Zonality of Te-bearing fahlore. Te-bearing fahlore is grey, light zones is composed of goldfieldite-tennantite-tetrahedrite (Tables 1, 2; anal. 2–17), dark zones are composed of golfieldite-tennantite and Te-bearing tennantite-tetrahedrite (Tables 1, 2; anal. 1, 18–27). Galena (gal) is white is galena, quartz (Q) is black (BSE-image). Sample 53/278, area 4.

Fig. 3. Grains of chalcopyrite, bournonite, and tetrahedrite filling intersitices between large (up to 100 microns) segregations of galena, sphalerite, and pyrite. (gal) Galena, (py) pyrite, (sph) sphalerite, (bour) bournonite, and (bl) fahlore. Digits correspond to numbers of analyses in Tables 6 and 7 for sulfides and bournonite, respectively (BSE-image). Sample 2, area 3.

fahlores occur as zoned crystals (Fig. 2). Zones are well distinguished by reflection and Te concentration. The light zones are goldfieldite-tennantite-tetrahedrite and goldfieldite-tetrahedrite-tennantite with Te content ranging from 6.63 to 13.52 wt.%; dark zones are goldfieldite-tetrahedrite-tennantite and Te-bearing tennantite-tetrahedrite with lower Te (up to 6 wt.%). In reflected light, Te-bearing fahlores are of pink tint; they are brighter than the other fahlores, weakly bireflected and hardly noticeable anisotropic. The intensity of pink tint is caused probably by the increasing Te in the composition. Rahmdor (1962) reported bireflectance and anisotropy of goldfieldite. The valence balance in fahlores containing more than 10 wt.% Te was calculated taking into account that the content of Cu^{+} in such minerals is more than 11 atoms, because surplus charge originating from substitution of Te^{4+} for $(As, Sb)^{3+}$ is compensated by depolarization due to reducing Cu^{3+} occupying vacancies in the framework to Cu^{+}. Mozgova and Tsepin (1983) made this point and it was confirmed by the study of the composition of Te-bearing fahlores from 11 volcanogenic and hydrothermal quartz-sulfide vein deposits of the gold-sulfide assemblage (Nenasheva, 2009). Belov (1952) noted the probable existence of Cu^{3+} in fahlore.

Tetrahedrite containing more than 4 wt.% Fe (up to 4.90) and significant Ag (2.88–4.87 wt.%), Zn (2.61–3.37 wt.%) is associated with pyrite, chalcopyrite, sphalerite, bournonite, hematite, copper sulfides (covellite, spionkopite, yarrowite, anilite, and geerite), tellurides (hessite, petzite, and altaite), and arsenates (leogangite and bayldonite) (Tables 1, 2; anal. 28–35). In some areas, such tetrahedrite fills interstices between grains of sphalerite, quartz, chalcopyrite, and galena. In the other areas, it together with bournonite fills interstices between quite coarse (up to 100 microns) grains of galena, sphalerite, and chalcopyrite (Fig. 3); in this case, grains of chalcopyrite are heterogeneous. Thin rims, small lamellas (1–2 microns in width), and point segregations of copper sulfides of the chalcocite polysomatic series (Fig. 4) are clearly observable in them.

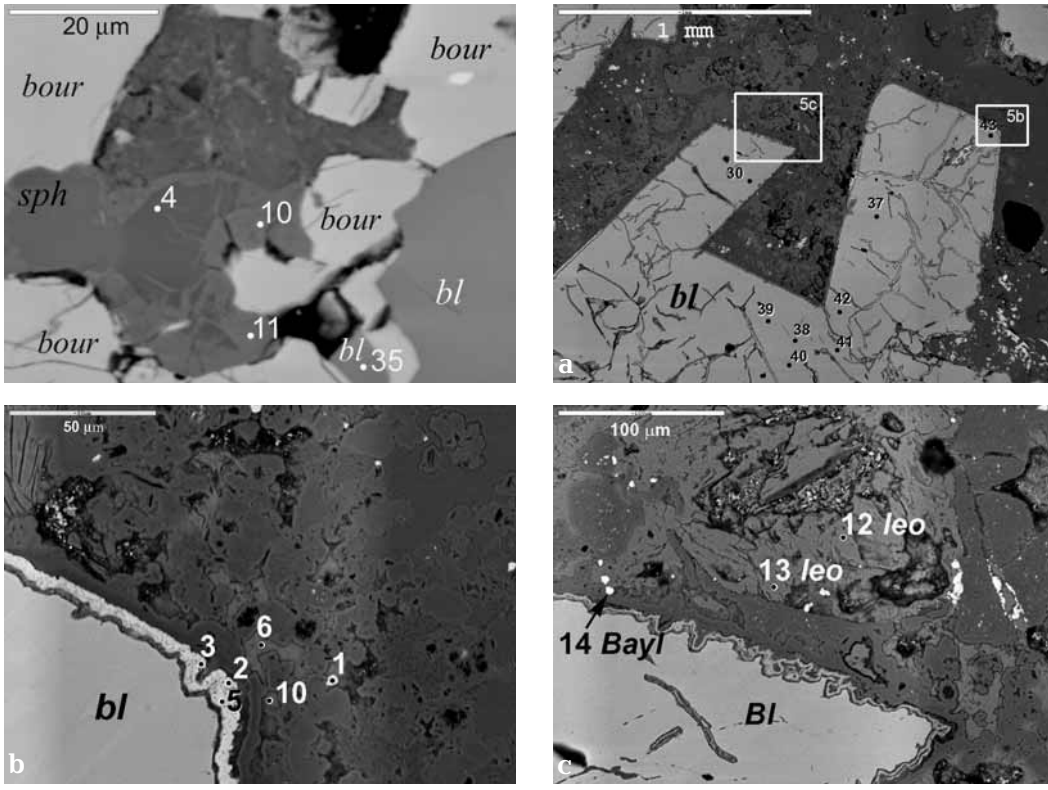

Fig. 4. Heterogeneous grains of chalcopyrite and copper sulfides of the chalcocite polysomatic series replacing chalcopyrite. (cp) Chalcopyrite, (an) anilite, (ge) geerite, (sp) spionkopite, (yar) yarrowite, (cov) covellite. Digits corresponds to numbers of analyses in Tables 6 and 1 for sulfides and fahlore, respectively (BSE-image). Sample 2, area 3.
Fig. 5. Large segregation of crinkly fractured anisotropic tennantite-tetrahedrite (light grey); the fractures are healed by secondary minerals: copper arsenates (darker tints of grey); (b, c) magnified fragments of selected areas. (bayl) Bayldonite, (leo) leogangite. Digits correspond to numbers of analyses in Tables 1, 4 (BSE-image). Sample 242/1-2.

Zn-rich tennantite-tetrahedrite (sandbergerite) differs from the aforementioned tetrahedrite, Te-bearing tetrahedrite-tennantite, and tennantite in brighter reflection like that of galena, visible bireflectance, and clear anisotropy (Tables 1, 2; anal. 36–43). In cross polars, it is well seen that sufficiently coarse grains are broken to the randomly oriented anhedral fine grains with different reflection allowing observation the bireflectance. Insignificant red inner reflections are observed in cross polars. Coarse segregations of this fahlore are broken crinkly fractures, which are healed by secondary minerals (Fig. 5), which are presumably arsenates; the latter was confirmed by reflections of euchroite and leogangite in the X-ray diffraction pattern of the fahlore (Table 3). The chemical composition of anisotropic fahlore corresponds to Zn-rich tetrahedrite-tennantite (sandbergerite). Anisotropic sandbergerite (Tables 1, 2; anal. 36–43) differs from isotropic once (Nenasheva *et al.*, 2010; Table 1; anal. 25–26) in the absence of admixture of Ag, Cd, and Pb. Tellurium that causes weak anisotropy of Te-bearing fahlores, is absent in anisotropic sandbergerite. The X-ray powder diffraction pattern of anisotropic tennantite-tetrahedrite (sandbergerite) (Table 3) is well consistent with that of tennantite given in the Peacock's atlas (Berry, Thompson, 1962). The unit cell dimension calculated on the basis of 12 reflections (Table 3; reflections nos. 5, 7, 8–13, 15–17, 19, and 20) is 10.1886 Å. In the X-ray powder diffraction pattern, there are reflections indexed in the unit cell of tennantite, but are absent in the X-ray powder diffraction pattern given in the Peacock's atlas (Table 3; reflections nos. 14, 29, 39, 41, 44, 47, and 57). It should be noted that many reflections of anisotropic tennantite-tetrahedrite are stronger in comparison with intensity of reflections

Table 3. **X-ray powder diffraction data of anisotropic Zn-rich tennantite-tetrahedrite**

	Sample 242/ 1-2 a = 10.1886 Å, V = 1057.5 Å^3			Tennantite T_d^3 – $I43m$, a = 10.21 Å Berry, Thompson, 1962				Bournonite a = 8.15, b = 8.70, c = 7.80 Å	Euchroite a = 10.05, b = 11.50, c = 6.11 Å Mikheev, 1957	Leogangite a = 21.77, b = 12.327, c = 10.72 Å, β = 92.85° Lengauer *et al.*, 2004
№	*I*	d_α(obs.)	d_α(calc.)	*hkl*	*hkl*	*I*	d_α(obs.)	d_α(pac.)	d_α(obs.) (I)	d_α(obs.) (I)	*d* (obs.) (I)
											10.85(10)
1	1	7.21	7.204	011						7.2 (10)	
2	0.5	5.46								5.8 (4)	5.44 (0.5)
3	0.5	5.16	5.094?	002?						5.2 (10)	
											4.9 (0.3)
4	3	4.43							4.37 (4)	5.00 (8)	
5	1	4.15	4.159	112	112	1	4.15	4.17	4.08 (3)	4.14 (4)	
6	3	3.90							3.90 (8)		
											3.728 (0.3)
7	2	3.62	3.602	022	022	0.5	3.60	3.61	3.68(2)	3.73 (8)	3.625 (0.5)
8	7	3.24	3.22	013	013	0.5	3.23	3.23	3.27(2)	3.29 (2)	
											3.09 (0.4)
9	10	2.94	2.941	222	222	10	2.94	2.95	2.99(4)	2.94 (7)	
10	1	2.82	2.826	023					2.82 (2)	2.81 (8)	
11	2	2.71	2.723	123	123	1	2.71	2.73	2.74 (10)	2.63 (7)	2.672 (0.4)
									2.69 (4)		2.63 (0.6))
12	7	2.54	2.547	004	004	3	2.55	2.55	2.59 (5)	2.55 (7)	
13	4	2.40	2.401	033	114,033	2	2.40	2.41	2.37 (1)	2.34 (6)	
14	1	2.29	2.278	024					2.30 (1)	2.26 (6)	
15	1	2.17	2.172	233	233	0.5	2.17	2.18	2.16 (0.5)	2.21 (5)	
16	2	2.08	2.080	224	224	0.5	2.07	2.08	2.09 (2)	2.07 (6)	
17	4	1.994	1.998	015,134	015,134	2	1.994	2.00	2.02 (0.5)	1.95 (7)	
									1.985 (3)		
18	2	1.907								1.90 (6)	
19	4	1.861	1.860	125	125	2	1.855	1.865	1.848 (4)	1.84 (6)	
20	8	1.803	1.801	044	044	8	1.801	1.807		1.78 (4)	
21	1	1.745	1.747	035,334	035,334	0.5	1.746	1.751	1.765 (6)	1.74 (4)	
22	2	1.696	1.698	006,244	006,244	0.5	1.695	1.702		1.71 (6)	
23	3	1.655	1.653	235,116	116,235	2	1.653	1.656	1.664 (2)	1.65 (7)	
24	1	1.612	1.611	026	026	0.5	1.608	1.615	1.631 (2)	1.61 (4)	1.618 (0.3)
25	0.5	1.590	1.591	045,344						1.562(5)	
26	1	1.569	1.572	154.145	145	0.5	1.568	1.576	1.556 (2)		
27	7	1.535	1.536	226	226	7	1.535	1.540		1.524 (4)	
28	0.5	1.516	1.519	036,245						1.513 (8)	
29	1	1.494	1.502	136							
30	2	1.473	1.471	444	444	1	1.467	1.475	1.480 (1)		
31	2	1.444	1.441	055,345,017	017,055,345	1	1.439	1.445		1.451 (7)	
32	0.5	1.425	1.427						1.427 (2)		
33	0.5	1.409	1.413	046						1.409 (4)	
34	1	1.386	1.386	127.255	336,255,127	0.5	1.386	1.390	1.389 (1)	1.385 (2)	
35	1	1.365	1.362	246	246	0.5	1.358	1.365	1.365 (1)		
36	1	1.297	1.294	156	237,156	0.5	1.296	1.297			
37	2	1.275	1.274	008	008	2	1.274	1.276			
38	1	1.258	1.254	018,147, 455	118,147, 455	0.5	1.254	1.257			
39	0.5	1.236	1.139	446,028							
40	2	1.220	1.218	356	356	1	1.217	1.220			
41	1	1.202	1.201	066							
42	3	1.185	1.184	057,347	138,057, 347	2	1.185	1.186			
43	4	1.169	1.169	266	266	3	1.169	1.171			
44	1	1.157	1.154	257							
45	1	1.142	1.139	048	048	1	1.139	1.141			
46	1	1.126	1.125	338,019	019,338, 129	0.5	1.126	1.128			
48	3	1.099	1.099	129,556,167	129,167, 556	1	1.100	1.101			
49	0.5	1.088	1.086	466	466	0.5	1.086	1.089			
50	1	1.077	1.074	158, 457	039,158,457	0.5	1.074	1.076			
51	0.5	1.068	1.068	139							
52	2	1.054	1.051	239, 367	239,367	0.5	1.052	1.054			
53	6	1.043	1.040	448	448	3	1.041	1.043			
54	2	1.032	1.034	566, 049							
55	1	1.024	1.024	177							
56	1	1.013	1.014	186,467,168							
57	1	1.003	0.999	268							
58	4	0.985	0.985	377, 666		2	0.980				
59	2	0.983									
60	4	0.976				1	0.970				
61	1	0.975									

Notes: The condition of reflection is h+k+l = 2n.

in the X-ray powder diffraction pattern given in the Peacock's atlas. It is explained by the superimposed strong reflections of euchroite $Cu_2(OH)[AsO_4]\cdot 3H_2O$ (Table 3; reflection nos. 3, 5, 7, 9, 11–13, 15–17, 19, 21–24, 31). According to the presence of reflections of euchroite in the X-ray powder diffraction pattern of anisotropic tennantite-tetrahedrite, euchroite got into preparation from crinkly fractures cutting the fahlore. The reflections (Table 3; nos. 2, 7, 11, and 24) in the X-ray powder diffraction pattern are probably caused by the admixture of leongangite $Cu_{10}^{2+}(OH)_6[AsO_4]_4[SO_4]\cdot 8H_2O$. In addition, indexing of twelve reflections (Table 3; reflection nos. 4, 6, 10, 18, 25, 28, 32, 51, 55, 56, 59, and 61) in dimensions of tennantite was failed. Reflections 10, 18, 25, and 28 belong to euchroite and reflections 4, 6, and 32 are attributed to bournonite, $CuPbSbS_3$. The assignment of high angle reflections (reflection nos. №№ 51, 55, 56, 59, 61) is not clear. The electron microprobe measurement of phases filling these factures was failed because the fractures are very narrow (about 1–2 microns, Fig. 6) and filling matter is heterogeneous. Optical properties of at least two phases are similar to arsenates, which immediately contact with anisotropic tennantite-tetrahedrite. These two phases occur as larger grains. In reflected light, one phase is light grey with weak light bluish tint and greenish yellow or yellowish orange translucence in chips; another phase is dark grey with greenish tint. In cross po-lars, the first phase is yellow-orange to brown, and the second phase is emerald-green. According to electron microprobe data, light grey phase with light bluish tint is bayldonite $PbCu_3(OH)_2[AsO_4]_2$ (Table 4; anal. 1–5, Fig. 6a), while dark grey phase with greenish tint is leogangite $Cu_{10}^{2+}(OH)_6[AsO_4]_4[SO_4]\cdot 8H_2O$ (Table 4; anal. 12–13, Fig. 6b). Thus, in the narrow fractures cutting grains of anisotropic tennantite-tetrahedrite, bournonite and three arsenates, bayldonite, leogangite, and euchroite $Cu_2(OH)[AsO_4]\cdot 3H_2O$, were identified. In addition, in the same sample, the other copper arsenates (duftite, clinotyrolite, strashimirite, clinoclase, and cornwallite), copper carbonate (azurite and malachite), and hematite were found with electron microprobe (Table 4).

Anisotropy of tennantite-tetrahedrite accounts for by pressure that results in crinkly fractures filled by copper arsenates, but the other explanations are probable.

Minerals associated with fahlores

As aforementioned, the fahlores studied are associated with varied minerals (Table 5). Nenasheva *et al.* (2010) reported chemical data and characteristic some of them: bornite, famatinite, sulvanite, arsenosulvanite, anglesite, tyrolite, clinotyrolite, and certain minerals of the chalcocite polysomatic series. The other phases are briefly characterized below.

The electron microprobe data of galena, pyrite, chalcopyrite, sphalerite, cubanite, and copper sulfides of the chalcocite polysomatic series (anilite, geerite, spionkopite, and yarrowite) are given in Table 6. In the second line of each analysis of galena, pyrite, chalcopyrite, and cubanite, the composition normalized to 100% for convenient comparison with theoretical composition are given. As seen from the table, compositions of galena and pyrite are close to theoretical. Chalcopyrite and cubanite were measured with well-shaped crystal (Fig. 6) occurred between grains of leogangite $Cu_{10}^{2+}(OH)_6[AsO_4]_4[SO_4]\cdot 8H_2O$. The crystal is heterogeneous. The areas of chalcopyrite and cubanite are distinguished. Within the crystal, chalcopyrite is chemically variable and contains lower sulfur (Table 6; anal. 5, 6, 7) in comparison with theoretical composition. The composition of cubanite is close to theoretical (Table 6; anal. 8, 9). The close intergrown chalcopyrite and cubanite indicate that the initial composition of the crystal corresponded to that of high-temperature solid solution of chalcopyrite (iss) identified experimentally at 350–300°C (Sugaki *et al.*, 1975). The exsolution at 250–300°C (Ramdohr, 1950) resulted in the formation of chalcopyrite variable in composition and cubanite.

Chalcopyrite and copper sulfides of the chalcocite polysomatic series associated with covellite and hematite fill interstices between grains of bournonite, galena, sphalerite, fahlore with thin rims, fine lamellas (1–2 microns in width), and point segregations of copper sulfides of the chalcocite polysomatic series being clearly observable in some grains of chalcopyrite (Fig. 3, 4). Electron microprobe measurements (Table 6; anal. 10–14)

Table 4. **Electron microprobe data (wt.%) of arsenates**

№ an.	Sample	Cu	Ag	Fe	Zn	Pb	As	Sb	V	S	Total
1	242/1-2	25.00	0.00	4.35	0.40	24.49	20,68	1.05		0.21	76.18
2		24.96	0.81	1.92	0.75	26.87	19.13	1.92		0.44	76.80
3		26.12	0.34	1.85	0.62	26.67	19.83	1.13		0.35	71.02
4		26.34	0.77	2.00	0.79	25.78	18.49	1.86		0.42	76.45
5		27.17	0.10	3.51	0.26	26.44	19.32	0.60		0.15	77.55
6		40.59		2.46	0.74		20.78	2.42		0.74	67.73
7	242/5 (area 1)	37.25					19.05		0.26	0.91	62.12
8		33.34		7.80			16.86		0.68	0.33	59.88
9		36.36		5.17			15.36		0.79	0.09	58.94
10	242/1-2	34.16	0.08	11.00	1.22	0.73	19.59	3.13		0.49	70.49
11		14.33		3.60	0.85	27.09	12.35				58.22
12		39.66	0.12	0.47	0.69	0.29	19,45	1.20		1.00	62.94
13		39.56	0.04	1.23	0.65	0.20	20.90	1.39		1.09	65.10
14	242/6 (area 1)	35.24		7.72			21.47	0.81	0.27	3.28	69.73

№ an.	Sample	Mineral and mixed minerals	Δ, % — valence balance
1	242/1-2	Bayldonite + hematite + arthurite	3.4
2		Bayldonite + hematite +	0.8
3		Bayldonite + hematite +	1.6
4		Bayldonite + hematite +	0.1
5		Bayldonite + hematite +	1.7
6		Strashimirite + hematite	0.3
7	242/5 (уч.1)	Clinotyirolite	1.6
8		Clinotyirolite + strashimirite + hematite	0.9
9		Clinotyirolite + cornwallite + hematite	1.1
10	242/1-2	Olivenite + hematite	0.8
11		Duftite + clinoclase	1.7
12		Leogangite	0.6
13		Leogangite	0.7
14	242/6 (area 1)	Leogangite + hematite	0.4

Notes: Including Ca (wt.%): anal. 7 — 0.94, anal. 10 — 4.65, anal. 11 — 0.87, anal. 12 — 1.17; and Mn (wt. %): anal. 8 — 0.06, anal. 9 — 0.04, anal. 13 — 0.09. Analyst L.A. Pautov; the compositions were recalculated by V.Yu. Karpenko.

Table 5. **Characteristic of fahlores and their assemblages**

№	Fahlore	Assemblage
1	Isotropic tetrahedrite with significant amount Zn-sandbergerite	Galena, chalcopyrite, pyrite, famatinite, sulvanite, anglesite, copper arsenates: bayldonite, leogangite, and euchroite.
2	Tetrahedrite-tennantite and tennantite	Galena, chalcopyrite, pyrite, sulvanite, arsenosulvanite, and Ca and Cu arsenates: tyrolite $Ca_2Cu_5^{2+}(OH,O)_4(AsO_4)_2(CO_3) \cdot 6H_2O$ or clinotyrolite $Ca_2Cu_9^{2+}(OH,O)_{10}[(AsO_4),(SO_4)]_4 \cdot 10H_2O$.
3	Anisotropic tennantite-tetrahedrite with sugnificant amount Zn-sandbergerite	Chalcopyrite, cubanite, grains of pyrite and galena partially replaced by secondary products including hematite and copper arsenates: bayldonite, leogangite, euchroite, duftite, clinotyrolite, strashimirite, clinoclase, and cornwallite. Veinlets of azurite and malachite are observable in specimens.
4	Tetrahedrite containing more than 4 wt.% Fe (up to 4.90 wt.%) and significant amount Ag (up to 4.87 wt.%) and Zn (up to 3.37 wt.%)	Pyrite, galena, chalcopyrite, sphalerite, bournonite, hematite, copper sulfides of the chalcocite polysomatic series $m Cu_2S \cdot n CuS$, tellurides (hessite, petzite, and altaite), arsenates (leogangite and bayldonite).
5	Goldfieldite-tennantite-tetrahedrite	Galena, pyrite, quartz, native gold, anglesite, secondary copper sulfides of the chalcocite polysomatic series $m Cu_2S \cdot n CuS$ (djurleite, digenite, roxbyite, anilite, geerite, spionkopite, and covellite).
6	Goldfeldite-tennantite	
7	Te-bearing tennantite-tetrahedrite	

Table 6. **Electron microprobe data (wt. %) of sulfides and sulfates**

№ an.	Sample	Mineral	Pb	Fe	Cu	Zn	S	Total	Formula	Δ, %
1	53/278 (area 7)	gal	85.40				13.19	98.59	$Pb_{0.99}S_{1.01}$	0.1
2	2 (area 3)	gal	86.36				13.28	99.64	$Pb_{1.00}S_{1.00}$	0.0
3	53/278 (area 7)	py	46.81				53.91	100.72	$FeS_{2.00}$	0.0
Theoretical chalcopyrite				30.43	34.63		34.94	100.00	$CuFeS_2$	
4	2 (area 3)	cp		27.91	33.51	2.03	33.65	97.10	$Cu_{1.00}Fe_{0.95}Zn_{0.06}S_{1.99}$	0.2
				28.74	34.51	2.09	34.65	100.00		
5	127/1	cp		28.90	32.37		33.85	95.12	$Cu_{0.98}Fe_{0.99}S_{2.03}$	2.7
				30.38	34.03		35.59	100.00		
6				30.04	32.54		34.083	96.66	$Cu_{0.97}Fe_{1.02}S_{2.01}$	0.2
				31.07	33.66		35.25	100.00		
7				29.50	33.10		34.33	96.93	$Cu_{0.98}Fe_{1.00}S_{2.02}$	1.5
				30.43	34.14		35.41	100.00		
Theoretical cubanite				41.20	23.40		35.40	100.00	$CuFe^{2+}Fe^{3+}S_{3.00}$	
8	127/1.			39.03	21.81		34.53	95.37	$Cu_{0.97}Fe^{2+}_{0.99}Fe^{3+}_{0.99}S_{3.05}$	2.9
				40.92	22.87		36.21	100.00		
9				41.32	23.98		34.70	100.00	$Cu_{1.03}Fe^{2+}_{1.01}Fe^{3+}_{1.01}S_{2.95}$	3.0
10	2 (area 3)	yar + sp	0.79		64.45		27.73	95.10	$(Cu_{16.53}Ag_{0.32}Pb_{0.06})_{16.91}S_{14.09}$	
									or $(Cu^{+}_{7.22}Ag_{0.32})_{7.54}Pb_{0.06}Cu^{2+}_{0.31}S_{14.09}$	
11	2 (area 3)	an + ge		2.00	72.58		23.40	97.97	$(Cu_{4.79}Fe_{0.15})_{4.94}S_{3.06}$ or	2.9
									$Cu^{+}_{3.94}(Cu^{2+}_{0.85}Fe_{0.15})_{1.00}S_{3.06}$	
12	2 (area 2)	yar		2.89	63.43		30.94	97.75	$Cu^{+}_{8.40}Ag_{0.04}Fe_{0.44}S_{8.12} \rightarrow$	2.9
									$(Cu_{1.96}Ag_{0.04})_{2.00}(Cu^{2+}_{6.44}Fe_{0.44})_{6.88}S_{8.12}$	
13	2 (area 2)	kov			65.23		32.98	98.22	$Cu_{0.999}S_{1.001}$	0.2
14					64.11		32.20	96.31	$Cu_{1.002}S_{0.998}$	0.4
15	2 (area 3)	sph		4.12		61.93	32.98	99.03	$(Zn_{0.92}Fe^{2+}_{0.07})_{0.99}S_{1.00}$	1.0
16	2 (area of fahlore)	sph		3.74	0.63	61.60	33.45	99.42	$(Zn_{0.91}Fe^{2+}_{0.06}Cu_{0.01})_{0.98}S_{1.01}$	3.0
17	53/278 (area 6)	angl	68.08				10.39	99.28	$Pb_{2.02}S_{1.99}O_{8.00}$ or $PbSO_4$	0.5

Notes: Δ, % — valence balance. * — including Ag (wt.%): 2.13 (anal. 10), 0.49 (anal. 12). Composition 17 anal. contains 20.81 wt.% O. Composition 2 anal. is average of two compositions. Composition 10 is attributed to the sample presenting mixure of yarrowite (72%) and spionkopite (28%). Legend: galena (gal), pyrite (py), chalcopyrite (cp), cubanite (cb), spionkopite (sp), yarrowite (yar), anilite (an), geerite (ge), covellite (cov), sphalerite (sph), and anglesite (angl). Analyst V.Yu. Karpenko.

revealed heterogeneity of these areas. The compositions 10 and 11 are calculated to electroneutral formula only assuming the examined grains are mixtures of yarrowite with spionkopite (anal. 10) and of anilite with geerite (anal. 11). The compositions 12–14 correspond to that of yarrowite (anal. 12) and covellite (anal. 13, 14). Electron microprobe data of hematite (49.97 wt.% Fe, 22.66 wt.% O, 1.05 wt.% S, total 73.42) are calculated to formula $Fe_{1.92}S_{0.05}O_{3.03}$. The presence of S accounts for the impurity of any sulfate phase $Fe^{3+}[SO_4]_3 \cdot nH_2O$. According to calculation, in this case, the formation of 0.05 molecules of $Fe^{3+}[SO_4]_3 \cdot nH_2O$ requires 0.1 atom of Fe^{3+} and 0.3 atom of oxygen. After residue of these amounts of Fe^{3+} and S, formula of hematite becomes neutral — $Fe_{1.82}O_{2.73}$ (valence balance — Δ, % = 0).

In this sample at adjacent area, more complex assemblage of galena, sphalerite, bournonite, hessite, petzite, altaite, and quartz is observed (Fig. 7a). The X-ray images of this area in the thin polished section are shown in Fig. 7b with well distinguishable grains of hessite ($AgL_{\alpha 1}$) and bournonite ($SbL_{\alpha 1}$). The electron microprobe data of sulfosalts and tellurides are given in Tables 7 and 8. In reflected light, bournonite is very similar to fahlore. It is light grey with greenish tint. Bireflectance and anisotropy are absent or extremely weak, so their documentation is impossible. The chemi-

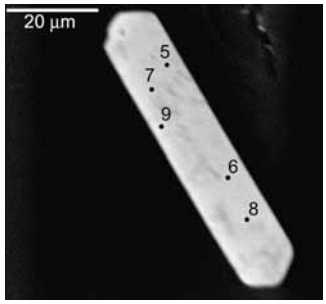

Fig. 6. Exsolved chalcopyrite crystal to form cubanite. Digits correspond to numbers of analyses in Table 6 (BSE-image). Sample 127/1.

cal composition of bournonite $PbCuSbS_3$ in the ore of the Lebedinoe deposits is as follows, wt.%: 41.09 – 42.44 Pb, 13.19 – 14.47 Cu, 22.68 – 24.78 Sb, 18.59 – 19.65 S (Tables 7, 8; anal. 1–10) that is weakly different from theoretical (42.54 Pb, 13.04 Cu, 24.65 Sb, 19.77 S).

The following telluride minerals were indentified: altaite, PbTe, hessite, Ag_2Te, and petzite, Ag_3AuTe_2. In reflected light, altaite is white, isotropic. According to electron micro-

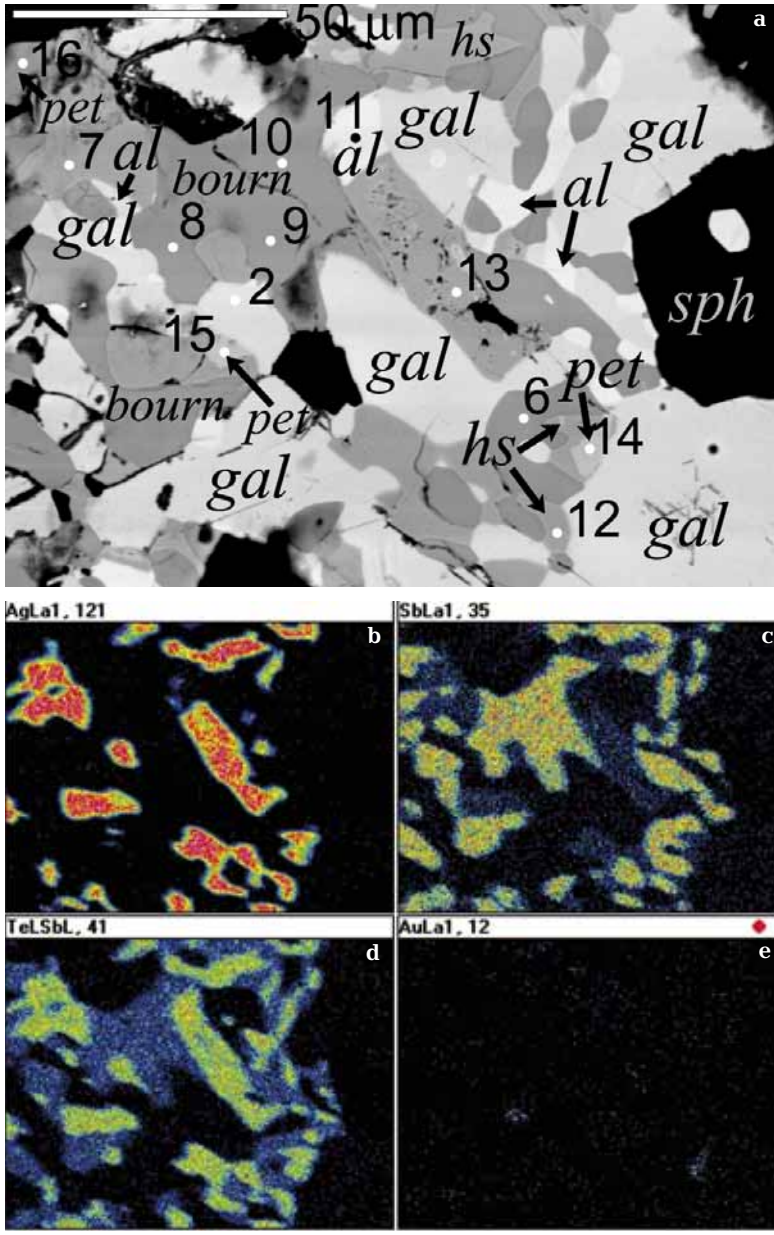

Fig. 7. Assemblage of galena (gal), sphalerite (sph), bournonite (bour), hessite (ges), petzite (pet), altaite (alt), and quartz (Q): (a) BSE-image, (b) X-ray elemental distribution map. Grains of hessite ($AgL\alpha_1$), bournonite ($SbL\alpha_1$) and hessite with bournonite ($TeL\alpha_1 + SbL\alpha_1$) are well distinguished. Digits correspond to numbers of analyses in Tables 6 and 7 for sulfides and bournonite, respectively. Sample 2, area 3.

Table 7. **Electron microprobe data (wt. %) of sulfosalts and tellurides**

№ an.	Mineral	Sample	Cu	Ag	Au	Zn	Sb	Pb	Te	S	Total
1	Bournonite	2 (area 3)	14.47				23.76	41.74		19.00	98.96
2			13.62			0.19	23.20	41.09		18.59	96.69
3			14.36			0.92	22.68	41.27		19.16	98.39
4			13.82				23.36	43.70		18.81	99.69
5			14.47			0.75	23.41	42.44		19.65	100.96
6			13.19				23.26	42.00		18.74	97.19
7			13.42				23.49	41.65		18.92	97.48
8			14.02				24.35	42.71		19.23	100.31
9			13.60				24.78	42.27		19.32	100.33
10			14.30				24.20	41.97		19.62	100.09
11	Altaite	2 (area 3)		3.32				59.84	36.74		99.90
								61.96*	38.04*		100.00*
12	Hessite	2 (area 3)		60.31			1.21		35.94		97.65
13				60.07			1.30		36.37		97.74
14	Petzite	2 (area 3)		42.53	21.87			1.10	32.66		98.00
15				41.13	22.53			1,08	32.48		97.22
16			0.66	40.44	22.78				31.39		95.27
Theoretical petzite				41.71	25.42				32.87		100.00

Notes: * *— After excluding Ag and normalization to 100 %. Including Se (wt. %): 0.36 (anal. 9), 0.20 (anal. 12) Composition 5 contains 0.24 wt. % As. Analyst V.Yu. Karpenko.*

Table 8. **Formulae of sulfosalts and tellurides**

№ an.	Mineral	Sample	Formula	Δ, % — valence balance
1	Bournonite	2 (area 3)	$Cu_{1.13}Pb_{0.99}Sb_{0.96}S_{2.92}$	2.5
2			$Cu_{1.08}Pb_{1.00}Sb_{0.96}S_{2.93}$	2.3
3			$Cu_{1.11}Zn_{0.07}Pb_{0.97}Sb_{0.91}S_{2.93}$	1.0
4			$Cu_{1.08}Pb_{1.05}Sb_{0.95}S_{2.92}$	3.0
5			$Cu_{1.09}(Pb_{0.98}Zn_{0.06})_{1.04}(Sb_{0.92}As_{0.02})_{0.94}S_{2.94}$	1.8
6			$Cu_{1.05}Pb_{1.03}Sb_{0.96}S_{2.96}$	1.3
7			$Cu_{1.06}Pb_{1.01}Sb_{0.96}S_{2.96}$	0.7
8			$Cu_{1.08}Pb_{1.01}Sb_{0.98}S_{2.93}$	2.8
9			$Cu_{1.04}Pb_{1.00}Sb_{0.99}(S_{2.94}Se_{0.02})_{2.96}$	1.5
10			$Cu_{1.09}Pb_{0.98}Sb_{0.96}S_{2.96}$	0.2
11	Altaite	2 (area 3)	$Pb_{0.95}Ag_{0.10}Te_{0.95}$	5.0
			or $Pb_{1.002}Te_{0.998}$ *	0.4*
12	Hessite	2 (area 3)	$(Ag_{1.96}Sb_{0.03})_{0.99}(Te_{0.99}Se_{0.02})_{1.01}$	1.5
13			$Ag_{1.96}Sb_{0.03}Te_{1.00}$	2.4
14	Petzite	2 (area 3)	$Ag_{3.09}Au_{0.87}Pb_{0.04}Te_{2.00}$	1.0
15			$Ag_{3.03}Au_{0.91}Pb_{0.04}Te_{2.02}$	0.5
16			$Ag_{3.01}Au_{0.93}Cu_{0.08}Te_{1.98}$	1.5

Notes: * *— After excluding Ag and normalization to 100 %.*

Table 9. **Minerals of the Cu-S system**

Mineral	Symmetry	Godovikov , Nenasheva, 2007		Gablina, 2008		
		Composition	Cu/S	Composition	Limit of thermal stability, °C	Products of phase transitions
Chalcocite high ↓ synthetic	Hexagonal	Cu_2S	2.000	Cu_2S	435	Digenite high
Chalcocite low ↓	Monoclinic	Cu_2S	1.993 − 2.001	$Cu_{1.993\text{-}2.001}S$	80 − 103	Chalcocite high
Tetrachalcocite ↓	Tetragonal	$Cu_{49}S_{25} \rightarrow Cu^{+}_{48}Cu^{2+}S_{25}$	1.960	$Cu_{1.96\text{-}2.0}S$	?	Digenite high
Djurleite ↓	Monoclinic	$Cu_{31}S_{16} \rightarrow Cu^{+}_{30}Cu^{2+}S_{16}$	1.938	$Cu_{1.93\text{-}1.96}S$	93 ± 2	Chalcocite low + digenite low
Roxbyite ↓	Monoclinic	$Cu_9S_5 \rightarrow Cu^{+}_{8}Cu^{2+}S_5$	1.800	$Cu_{1.72\text{-}1.82}S$	50 − 90	
Digenite high ↓	Cubic	Cu_2S	2.000	Cu_2S	>1000	Melt
Digenite low ↓	Trigonal, pseudo-cubic	$Cu_9S_5 \rightarrow Cu^{+}_{8}Cu^{2+}S_5$	1.800	$Cu_{1.75\text{-}1.78}S$	75 − 83	Digenite high
Anilite ↓	Rhombic	$Cu_7S_4 \rightarrow Cu^{+}_{6}Cu^{2+}S_4$	1.750	$Cu_{1.75}S$	30 − 75	Digenite low
Geerite ↓	Trigonal	$Cu_3S_2 \rightarrow Cu^{+}_{2}Cu^{2+}S_2$	1.500	$Cu_{1.5\text{-}1.6}S$	?	?
Spionkopite ↓	Hexagonal	$Cu_{39}S_{28} \rightarrow Cu^{+}_{22}Cu^{2+}_{17}S_{28}$	1.393	$Cu_{1.4}S$	157	Covellite
Yarrowite ↓	Hexagonal	$Cu_9S_8 \rightarrow Cu^{+}_{2}Cu^{2+}_{7}S_8$	1.125	$Cu_{1.1}S$	157	Covellite
Covellite ↓	Hexagonal	$3CuS \rightarrow Cu^{+}_{2}S \cdot Cu^{2+}[S_2]$	1.000	CuS	507	Digenite
X-bornite				$Cu_{5\text{-}x}FeS_4$	75 − 140	Chalcopyrite + bornite

Notes: Arrows indicates pH decreasing, copper realizing, and increasing importance of bivalent copper.

probe measurements, the mineral contains 3.32 wt.% Ag (Tables. 7, 8; anal. 11). According to handbook edited by Bonshtedt-Kupletskya, few Ag in altaite occurs as admixture. Ag in altaite from the Stepnyak gold deposit (Kazakhstan) belong to native silver (Minerals, 1960). Carrier of Ag in altaite from the Kalgoorlie deposit is aguilarite (Ramdohr, 1962). Altaite from the Lebedinoe deposit occurs as grains of 5 − 10 microns in size, which being magnified 825 times in microscope look homogeneous; the association is similar to that in the Stepnyak deposit; neither Se nor S were detected, therefore it can be concluded that Ag in altaite occurs as tiny inclusions of native silver. This admixture probably explains the non-uncharged formula of altaite with good sum of elements 99.90 wt.%. If Ag is excluded than formula becomes uncharged (balance valence is 0.4%).

Hessite is present as tiny elongate grains (Figs. 7a, 7b). The reflection is high similar to galena. Bireflectance is very weak; anisotropy ranges from light grey with cream tint to light grey with light bluish tint. The composition (Tables 7, 8; anal. 12, 13) is close to theoretical (Ag 62.86, Te 37.14 wt.%), but admixture of Sb slightly greater than 1 wt.% and Se 0.2 wt.% was detected.

The composition of petzite Ag_3AuTe_2 is also close to theoretical (Tables 7, 8; anal. 14 − 16). With well relation of components (electroneutrality of formulae < 1.5), the compositions have lowered total (lowered gold content) that accounts for by small size of grains ~ 3 − 5 microns. In reflected light, petzite is hardly brighter hessite; it is isotropic, greyish white.

Discussion

Thus, fahlores of the Lebedinoe deposit are extremely varied in: (1) character of univalent metals (in addition to Cu, Cu-Ag were identified); (2) elemental set of bivalent metals (Zn, Zn-Fe, Fe-Zn, Cu-Fe, and Cu-Zn); and (3) character of semimetals (significantly Sb, Sb-As, As-Sb, Sb-As-Te). They were estab-

lished in various assemblages (Table 5). Galena, chalcopyrite, pyrite, and copper arsenates were found in all assemblages.

In addition, in assemblage no. 1 (Table 5), isotropic sandbergerite is associated with famatinite, sulvanite, anglesite, and copper arsenates: bayldonite, euchroite, and leogangite. According to Betekhtin (1950), anglesite is formed in the cementation zone of the deposits containing copper sulfides in addition to lead and zinc sulfides and in the oxidizing zone of Pb-Zn sulfide deposits. The temperature of formation of this assemblage can be higher 250–300°C.

The assemblage of tetrahedrite-tennantite and tennantite with sulvanite, arsenosulvanite, and Ca and Cu arsenates (tyrolite and clinotyrolite) is the next (Table 5; no. 2). Sulvanite indicates introduction of arsenic in mineralizing fluid.

Anisotropic tennantite-tetrahedrite (Table 5; no. 3) is associated with chalcopyrite, cubanite, pyrite, and galena partly replaced by arsenates: bayldonite, leogangite, euchroite, duftite, clinotyrolite, clinoclase, strashimirite, and cornwallite. Close intergrown chalcopyrite and cubanite testify to high-temperature exsolution of chalcopyrite at 250–300°C (Ramdohr, 1950) indicating lowering temperature of formation of the described ores.

The assemblage of tetrahedrite (Table 5; no. 4) containing > 4 wt.% Fe (up to 4.90) and significant Ag (up to 4.87 wt.%) and Zn (up to 3.37 wt.%), bournonite, tellurides (hessite, petzite, and altaite), hematite, copper sulfides of the chalcocite polysomatic series $m Cu_2S \cdot n CuS$, and arsenates (leogangite and bayldonite) resulted from next change of mineral-forming conditions, introduction of Ag, Fe, and Te in mineralizing fluid, and temperature decreasing below 155°C, that is indicated by anisotropic hessite AgTe, which transforms to cubic modification at 155°C (Minerals, 1960). It is notable that tetrahedrite in this assemblage is Te-free. Probably, Te is used up the formation of hessite, petzite, and altaite.

Later generation of fahlore contains significant Te. At the Lebedinoe deposit, Te-bearing fahlores are identified in association with copper sulfides of the chalcocite polysomatic series with tellurides (hessite, petzite, and altaite) being absent. Tellurium species are transforming that was previously reported in assemblages of the Kochbulak deposit (Kavalenker *et al.*, 1980).

The immediate contact of yarrowite (Table 6; anal. 15) and covellite (Table 6; anal. 13, 14), which are the Cu-poorest copper sulfides, testifies to the acidic mineral-forming environment, because these minerals are formed in acidic medium (Gablina, 1997). This is supported by the high activity of Cu and As, and copper arsenates in the ores which are stable in acidic, neutral, and weakly alkaline medium (pH 2.5–8.7). With the background activity of Cu and As, copper arsenates are not formed (Charykova *et al.*, 2010). Yarrowite and spionkopite are stable up to 157°C (Table 9). Finding of mixed anilite and geerite (Table 6; ansl. 11) is testimony to the formation temperature below 75°C , because at this temperature anilite transforms to low-temperature digenite (Table 9). Unfortunately, the data of the stability field of geerite are absent.

The finding of hematite associated with copper sulfides and anisotropic tetrahedrite-tennantite contradicts the statement by Fastalovich and Petrovskaya (1940) that "hematite is never found with minerals of polymetalic assemblage".

Thus, two mineral species (tennantite and tetrahedrite) according to nomenclature of fahlores suggested by Mozgova nad Tsepin (1984), were identified in the ores of the Lebedinoe deposit, among them five varieties (tennantite-tetrahedrite, goldfieldite-tennantite-tetrahedrite, goldfieldite-tetrahedrite-tennantite, Te-bearing tennantite-tetrahedrite, and Te-bearing tetrahedrite-tennantite) were distinguished. Such diversity is caused by change of mineral formation conditions: change of the composition of ore-forming hydrothermal fluids, decreasing temperature of formation, changing of redox potential and pH of mineral-forming medium.

Financial support was provided by Ministry of Education and Science of Russian Federation through grant № 16.518.11.7101.

References

Belov N.V. Essay about structural mineralogy. Part III. Collected mineralogical articles. Lvov Geol. Soc. **1952**, No. 6. P. 21–34 (in Russian).

Berry L.G., Thompson R.M. X-ray powder data for ore minerals: the Peacock atlas. New York. **1962**. 313 p.

Betekhtin A.G. Mineralogy. Moscow: Gosgeolizdat, **1950.** 956 p. (in Russian).

Charykova M.V., Krivovichev V.G., Yakovenko O.S., Depmeir W. Thermodynamics of arsenates, selenites, and sulfates in the oxidation zone of sulfide ores: III. Diagrams Eh-pH of the Me-As-H_2O systems (Me = Co, Ni, Fe, Cu, Zn, Pb) at 25°C. // Zap. VMO. **2010**. Pt CXXXIX, No. 3. P. 1–14 (in Russian).

Fastalovich A.I., Petrovskaya N.V. The type of mineralization of the Lebedinoe gold deposit, Aldan. // Sov. Geologiya. **1940**, No. 2–3. P. 64–65 (in Russian).

Gablina I.F. Copper sulfides as indicators of the ore-forming environment. // Dokl. Earth Science, **1997**. Vol. 357. P. 1133–1137 (in Russian).

Gablina I.F. Copper and copper-iron sulfides as indicators of conditions of formation and transformation. **2008**. RMS DPI 2008-2-10-0, www.minsoc.ru/FilesBase/2008-2-10-0 (in Russian).

Kovalenker V.A., Troneva N.V., Dobronichenko V.V. Peculirities of composition of the main ore-forming minerals from tube-like ore bodies at the Kochbulak deposit. In: Methods of investigation of ore-forming minerals and their assemblages. Moscow: Nauka, **1980**. P. 140–164 (in Russian).

Lengauer C.L., Giester G., Kirchner E. Leogangite, $Cu_{10}(AsO_4)_4(SO_4)(OH)_6{\cdot}8H_2O$, a new mineral from the Leogang mining district, Salzburg province, Austria // Mineralogy and Petrology. **2004**. 81. P. 187–201.

Mikheev V.I. X-ray identification of minerals. Moscow: Gosgeotekhizdat, **1957**. 868 p. (in Russian).

Minerals. Moscow: AN SSSR Press, **1960**. Vol. 1, 617 p. (in Russian).

Mozgova N.N., Tsepin A.I. Fahlores. Moscow: Nauka, **1983**. 280 p. (in Russian).

Nenasheva S.N. Peculiarities of composition of Te-bearing fahlores. //New Data on Minerals. **2009**. Vol. 44. P. 34–44.

Nenasheva S.N., Karpenko V.Yu., Pautov L.A. Sulfide mineralization of the Lebedinoe deposit, Central Aldan. // New Data on Minerals. **2010**. Vol. 45. P. 60–66.

Petrovskaya N.V. Native gold. Moscow: Nauka, **1973**. 347 p. (in Russian).

Ramdohr P. Die Erzmineralien und ihre Verwachsungen. Akademie-Verlag Berlin. **1950**.

Sugaki A., Sgima H., Kitakaze A., Harada H. Isothermal phase relations in the system Cu-Fe-S unger hydrotermal conditions at 350°C and 300°C // Econ. Geol. **1975**. V. 70. P. 806–823.